Solar Energy Materials and Solar Cells 185 (2018) 517–523

Contents lists available at ScienceDirect

Solar Energy Materials and Solar Cells

journal homepage: www.elsevier.com/locate/solmat

Anti-soiling coatings for solar cell cover glass: Climate and surface properties influence

Magnum Augusto Moraes Lopes de Jesus[a], Gianluca Timò[b], Cecilia Agustín-Sáenz[c], Iñigo Braceras[c], Marina Cornelli[b], Angela de Mello Ferreira[d,e,*]

[a] Department of Chemistry - Universidade Federal de Minas Gerais (UFMG), Belo Horizonte, Minas Gerais, Brazil
[b] Materials and Generation Technologies Department, Ricerca sul Sistema Energetico – RSE, Piacenza, Italy
[c] Energy and Environment Division - TECNALIA - Parque Científico y Tecnológico de Gipuzkoa, Mikeletegi Pasealekua 2, Donostia - San Sebastián, Spain
[d] Department of Chemistry - Centro Federal de Educação Tecnológica de Minas Gerais (CEFET-MG), Belo Horizonte, Minas Gerais, Brazil
[e] National Institute of Science and Technology on Mineral Resources, Water and Biodiversity, (INCT- Acqua), Brazil

ARTICLE INFO

Keywords:
TiO_2/SiO_2 films
Hydrophilic/hydrophobic self-cleaning surfaces
Anti-soiling coatings
Climate influence
Solar cell cover glass

ABSTRACT

The objective of this study has been twofold: i) to investigate different strategies for CPV module glass surface modification, in particular preparing hydrophilic and hydrophobic coatings in order to reduce the dust accumulation (soiling) on the module surface; ii) to perform a joint comparative soiling testing in Italy, Spain and Brazil in order to understand the limit and advantages of the proposed anti-soiling coatings in different climate condition. Two TiO_2/SiO_2 films with different titanium content have been synthesized and benchmarked against pure TiO_2 in relation to transparency and hydrophilicity. Moreover, a hydrophobic antireflective material based on functionalized-SiO_2 thin film was also investigated. All these coatings have been deposited over low iron float glass substrates by sol-gel dip-coating and electron-beam evaporation technique. TiO_2/SiO_2 and functionalized-SiO_2 films showed higher transmittance in visible range than pure TiO_2. TiO_2/SiO_2 films showed a persistent superhydrophilic character with water contact angles near to 0°, while functionalized-SiO_2 presented hydrophobic property. The joint comparative soiling tests showed the importance of setting anti-soiling strategies in region characterized by more dry climate: in Brazil, which during the soiling test was characterized by a long dry period, the anti-soiling coatings were effective in reducing the soiling deposition and in the removal of the contaminants by rainwater; in Spain and Italy, the more frequent rain precipitation made the soiling effect less relevant, however, the deposition of anti-soiling coating on the module cover glass allowed to fully recover the initial transmittance after rain washing. A chemical and mineral characterization of the soiling has been carried out revealing the dependence of the contaminants from the environment conditions (e.g. car traffic, presence of industries, amount of rain and local minerals in the ground).

1. Introduction

The development of technologies for renewable energy is essential in the current world scenario that presents environmental problems and a shortage of fossil resources. The photovoltaic (PV) technologies stand out because they are renewable, safe and eco-friendly sources of electrical power [1]. Nowadays in order to increase the PV energy production the technological efforts are not only driven towards the development of high PV performance and reliable solar cells but also towards the means to mitigate the external factors that can reduce the conversion efficiency of the PV modules. One of these factors is the soiling effect caused by dust accumulation on module surface that reduces the transparency of the PV cover glass over time and consequently decreases the module PV energy production [2]. Dust usually deposits on the surface of the module cover glass as a thin layer of particles with less than 10 μm in diameter and its accumulation has a great dependence with the location/environment condition [2]. Soiling deposition on PV modules has been widely studied in literature [2–7], however, most contributions analyze the effect of dust accumulation in reducing the efficiency of PV modules or the transmission of glass

Abbreviations: CPV, concentrator photovoltaic; PV, photovoltaic; LIFG, low iron float glass; TIPT, titanium isopropoxide; TEOS, tetraethyl orthosilicate; SDA, structure-directing agent; UV–Vis–NIR, ultraviolet-visible-near-infrared; BEMA, Bruggeman effective medium approximation; WCA, water contact angle; RMS, root mean square; AFM, atomic force microscopy; SEM, scanning electron microscope; EDS, energy disperse spectroscopy

* Corresponding author at: Department of Chemistry - Centro Federal de Educação Tecnológica de Minas Gerais (CEFET-MG), Av Amazonas, 5253, 30.421-169 Belo Horizonte, Minas Gerais, Brazil.
E-mail address: angelamello@cefetmg.br (A.M. Ferreira).

https://doi.org/10.1016/j.solmat.2018.05.036
Received 4 December 2017; Received in revised form 20 April 2018; Accepted 15 May 2018

modules, while only fewer ones have evaluated different alternatives of anti-soiling coatings by testing them in different environmental outdoor conditions [8–11]. The possibility to prevent the soiling deposition is accomplished by the modification of the module glass with a self-cleaning and/or "easy to clean" surface [9]. Self-cleaning effect can be obtained by the deposition of TiO_2 thin films on cover glass. This material offers both photocatalysis, which is responsible of the decomposition of organic contaminants, and photo-induced superhydrophilicity, that makes easier the washing of the contaminants from the surface by rainwater [12]. However, TiO_2 reduces the glass transmittance and it rapidly loses the hydrophilicity, re-establishing the water contact angle in dark environments. TiO_2/SiO_2 composite films can overcome all these limitations [13]. TiO_2/SiO_2 films present high transmittance, enhanced photocatalytic activity and persistent superhydrophilicity in dark environments [1,13–17]. These coatings can be promising also for concentrating photovoltaic (CPV) applications whose modules make use of multijunction solar cells, and therefore need transparent anti-soiling coating in a wide wavelength region (typically between 300 and 1800 nm). "Easy to clean" surfaces can be obtained, for example, by hydrophobic functionalized silica, since this film has the property to produce moving spherical water drops which can collect the dust particles and eventually flow off the surface [9,18–20]. In this work, anti-soiling coatings based on TiO_2, TiO_2/SiO_2, and fuctionalized-SiO_2 films have been deposited on glass, characterized regarding their optical and structural properties and then compared in their performance in preventing the soiling deposition. The morphology and composition of the deposited dust has been analyzed and soiling dependence on weather conditions (humidity, rain precipitation) assessed. The soiling test has been performed in different locations, in particular in Italy, Spain and Brazil in order to understand the limits and advantages of the proposed self-cleaning surfaces under the different climate conditions.

2. Experimental details

2.1. Coatings preparation

The anti-soiling coatings used in this work were obtained by sol-gel and electron beam evaporation (e-beam) methods and were deposited at low iron float glass (LIFG, Pilkington Optiwhite Low Iron) substrates.

2.1.1. Superhydrophilic sol-gel TiO_2/SiO_2

These composite films were obtained by previous established procedure [13]. LIFG substrates 4 mm thick were ultrasonically cleaned with ethanol (EtOH) and air dried. TiO_2 precursor solution was prepared using titanium isopropoxide (TIPT), isopropanol (IspOH) (99% w/w) and water (H_2O) with TIPT:IspOH:H_2O molar ratio equal to 1:97:0.5. Similarly, SiO_2 precursor solution was prepared using tetraethyl orthosilicate (TEOS) with TEOS:IspOH:H_2O molar ratio equal to 1:47:2. TiO_2/SiO_2 composite films were prepared with different Si/Ti molar rate mixed solutions. The abbreviations $Si_{86}Ti_{14}$ and $Si_{40}Ti_{60}$ mean the Si/Ti molar rate used to prepare the TiO_2/SiO_2 composite films by the mixture of SiO_2 and TiO_2 precursor solutions. One side of the glass was recovered with the film using the dip-coating equipment Marconi (MA 765) at room conditions (20 °C, relative air humidity lower than 30%) with a withdraw speed of 3.6 mm/s. Then, films were treated in muffle furnace at 500 °C for 2 h under air $Si_{86}Ti_{14}$ composite film is referred in this study as ST1 sample while the $Si_{40}Ti_{60}$ film as ST2 sample.

2.1.2. Superhydrophilic e-beam TiO_2

As a benchmark, TiO_2 film sample was deposited onto one side of the glass by e-beam evaporator Kenosistec® UHV Thin Film Equipament - using solid Kurt J. Lesker® TiO_2 - USA, 99.99% purity and particle size of 1–4 mm. This TiO_2 film was referred as T sample.

2.1.3. Hydrophobic sol-gel SiO_2

These films consisted of multilayer stacks of graded refractive index SiO_2 sol-gel films deposited by dip-coating technique and functionalized by an 'easy to clean' post-treatment based on silylating agents to provide the hydrophobicity. The substrates were ultrasonically cleaned with ethanol (EtOH) and air dried. Tetraethyl orthosilicate (TEOS), poly (oxyethylene) cetyl ether, and ethanol (EtOH) (99%w/w) were used as precursor, structure-directing agent (SDA) and solvent for sol-gel solution. Two different sols containing or not SDA were prepared in order to obtain multi-layer stack composed by films with different refractive indexes. The multi-layer stack is composed by an inner denser (D) film of higher refractive index and an external porous (P) film of lower refractive index. Film deposition was performed onto one side of the glass substrate using homemade dip-coating equipment at controlled conditions (22 °C, relative air humidity 60%). LIFG substrates were first immersed and emerged in the non-containing SDA sol-gel with a speed of 0.83 mm/s and then films were treated in muffle furnace at 550 °C for 1 h under air. Subsequently these coated substrates were immersed and emerged in the containing SDA sol-gel with a speed of 0.83 mm/s and were treated in muffle furnace at 550 °C for 1 h under air. A post-treatment with hexamethyldisilazane (H) solution was then performed. This silylating treatment allows reducing the number of free silanol groups (Si-OH) in the surface and substituting them by methyl groups attached to Si thus permitting to obtain hydrophobic surface, the obtained sample was referred in this study as SM sample (Patent EP17382016) [21].

All samples prepared in this work are summarized in Table 1.

2.2. Characterization of the coatings

Transmittance (%T) spectra were measured with a UV–Vis–NIR spectrophotometer Jasco V-670 (with integrating sphere) in 300–2000 nm wavelength. Integrated transmittance was calculated by weighting transmittance values with mean hemispherical solar spectral irradiance incident on surface tilted 37° toward the sun (ASTM G173-03) according to equation:

$$\tau = \frac{\int_{\lambda_1}^{\lambda_2} T_\lambda \cdot S_\lambda \, d\lambda}{\int_{\lambda_1}^{\lambda_2} S_\lambda \, d\lambda} \quad (1)$$

Where T_λ is the transmittance spectrum of the covered glass, S_λ is the hemispherical solar spectral irradiance for absolute air mass of 1.5 (ASTM G173-03) and λ_1 and λ_2 define the wavelength range in which τ is calculated.

Ellipsometric parameters ψ and Δ of the SM film were recorded by Variable Angle spectroscopic ellipsometer. Spectra were recorded at wavelength comprised from 300 nm to 1000 nm at three angles of incidence (65°, 70°, 75°). The data analysis was performed with WVase32 software. The spectra were fitted using the dispersion Cauchy model for obtaining spectral refractive index n and film thickness. The Bruggeman effective medium approximation (BEMA) model was adopted for void fraction calculation. The void fraction of each film was calculated considering polarization factor of 0.33 with respect to pure dense silica, thus value of absolute porosity in % was provided.

A VARIAN CARY 50 spectrophotometer was used in the soiling test and the transmittance was measured in the range of 200–1100 nm. An

Table 1
List of samples prepared with their composition and classification.

Sample references	Composition	Classification
ST1	$Si_{86}Ti_{14}$	Hydrophilic
ST2	$Si_{40}Ti_{60}$	Hydrophilic
T	TiO_2	Hydrophilic
SM	Functionalized-SiO_2 bi-layer	Hydrophobic

average transmittance in 300–1100 nm wavelength was used to analyze transmittance variations of the coatings during the soiling test. Water contact angle (WCA) measurements were assessed by KRUSS DS100 goniometer (connected to a video camera) to evaluate the surface hydrophilicity/hydrophobicity. These measurements were made at 25 °C and relative air humidity lower than 50%. Deionized water droplets volume was fixed at 2 μL and was used 2 drops per sample and 3 replicates. Raman spectra were obtained on a Horiba Jobin Yvon LABRAM-HR 800 spectrograph, equipped with a 633 nm helium-neon laser, frequency range of 100–800 cm^{-1}, 20 mW of power, attached to an Olympus BHX microscope equipped with 10, 50, and 100 × lenses. For dust characterization, the laser power was 0.08 mW and frequency range of 100–2000 cm^{-1}. The acquisition time was 60 s, with a number of samples equal to 10. T, ST1 and ST2 thicknesses were measured by an atomic force microscope (AFM) Asylum Research - MFP-3D in tapping mode. Root mean square (RMS) roughness values were obtained by spectral analysis on 1 μm^2 areas.

2.3. Soiling test method

Glasses samples containing different anti-soiling coatings (hydrophobic or superhydrophilic) have been installed outdoor beside the CPV modules, as seen in Fig. 1 in three different locations: San Sebastián city-Spain, Belo Horizonte city-Brazil, and at Piacenza city-Italy. Soiling test has been carried out in a period of between 4 and 5 months. Every two 2 weeks the glass samples have been analyzed by transmittance measurement in order to check the dust accumulation.

3. Results and discussion

3.1. Anti-soiling coating characterization

Fig. 2 shows the transmittance spectra of the different anti-soiling coatings in wavelength range 300–2200 nm before soiling exposition. Table 2 shows the integrated and gained transmittances of the anti-soiling coatings, in the mentioned wavelength range, with respect to an uncoated glass (bare glass substrate).

SM sample has been designed also to present anti-reflective property, since it is an import requirement for their application as solar cell cover glass [8,15,20]. SM showed a gain in visible-near-infrared range of about 3%, over bare substrate. The control of thickness and refractive index of SiO_2 layers leads to this increase of transmittance, as will be further discussed in ellipsometric results. ST1 and ST2 samples haven't showed anti-reflective properties, however have presented good %T (~88–89%) in visible-near-infrared range, which is comparable to the transmittance of the bare substrate. These coatings can confer anti-soiling effect to the glass surface without compromising the transmittance, which is fundamental for photovoltaic application. The benchmark sample T presented the lowest transmittance (~72%) due to the sub-bandgap absorption at 500–1600 nm. This sub-bandgap absorption of the sample T, is due to its higher thickness (100 nm) than the ones prepared by sol –gel (63 nm (ST2) and 85 nm (ST1)). Besides this,

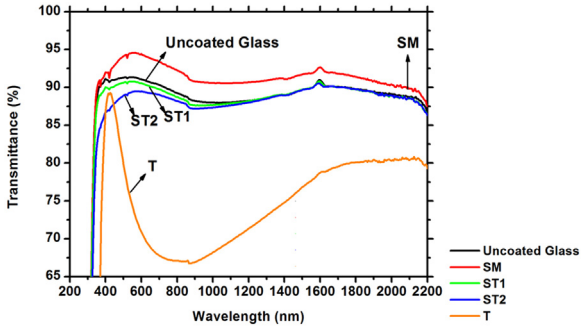

Fig. 2. % Transmittance spectra of anti-soiling coatings before soiling exposition.

Table 2
Integrated and gained transmittance of anti-soiling coated glasses and bare glass substrate in the range 300–2200 nm.

Sample	T	ST1	ST2	SM	Bare low iron float glass
%T (300–2200 nm)	72.1	89.2	88.1	92.3	89.7
Gain over the bare glass substrat % (300–2200 nm)	−19.7	−0.6	−1.8	2.8	–

Sample T has the highest refractive index (pure TiO2) among the samples, therefore the highest reflection.

It is possible to notice that ST1 and ST2 are based on TiO_2/SiO_2 films and showed an important transmittance improvement compared to T, owing to hybrid nature of the film.

As superhydrophilicity and hydrophobicity are fundamental to give a self-cleaning property to the glass [9,12,18–20], water contact angles (WCA) measurements of all coatings were performed before and after UV irradiation for 30 min, as seen in Table 3. SM sample has presented hydrophobic property (angle > 90°), as expected as it has been functionalized with hydrophobic compound. WCA of SM was not measured after UV irradiation, because this coating has not photocatalytic property. After 30 min of UV irradiation, T, ST1 and ST2 have presented superhydrophilic property (angle < 5°), except uncoated glass, showing how this glass modification is efficient to give superhydrophilic property to this material. This behavior can be explained by the photocatalytic property due to anatase phase. WCA measurements were performed with 3 months of aging and the results of the superhydrophilic state of ST1 and ST2 were similar [13]. The mixture of SiO_2 on TiO_2 results in a generation of Bronsted acidity that increases the number of hydroxyl groups, giving to the surface a superhydrophilic property. These groups trap the photogenerated holes and retard the electron-hole recombination [22]. The charge of electrons and holes can favor a molecular or dissociative adsorption of water on the surface of TiO_2/SiO_2 that results in a natural and persistent superhydrophilicity even at dark environments [23]. T did not preserve WCA < 5° after 2

Fig. 1. Soiling test facility: solar tracker (left) and the sample holder (right).

Table 3
Water contact angles (WCA) before and after ultraviolet irradiation for 30 min.

Sample	T	ST1	ST2	SM	Uncoated glass
Before UV (°)	(62.0 ± 0.2)	(1.0 ± 0.1)	(1.0 ± 0.1)	(95.4 ± 1.6)	(30.0 ± 0.2)
After UV (°)	(4.0 ± 0.2)	(0.1 ± 0.1)	(0.1 ± 0.1)	–	(30.0 ± 0,2)

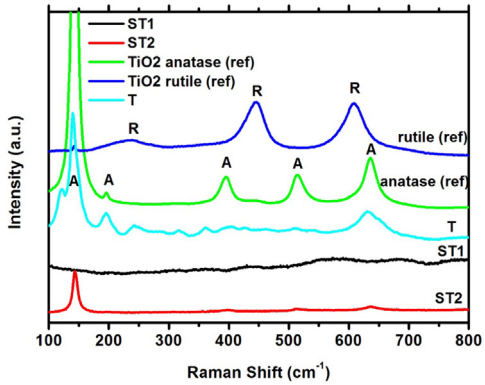

Fig. 3. Raman spectra of T, ST1 and ST2 anti-soiling coatings.

weeks (in the darkness), whereas ST1 and ST2 did. At dark environments, pure TiO_2 films tends to re-establish the hydrophobicity quickly, while TiO_2/SiO_2 composite films slows down this reestablishment [13,14,17,23].

T, ST1 and ST2 samples have been characterized by analyzing their crystalline phases, while SM has been characterized by analyzing its thickness, refractive index and porosity.

Raman spectroscopy was used to characterize titanium phases in T, ST1 and ST2 coatings, as shown in Fig. 3. TiO_2 anatase Raman modes are: E_g at 143 cm^{-1}/196 cm^{-1}, B_{1g} at 393 cm^{-1}, A_{1g}/B_{1g} at 514 cm^{-1} and E_g at 639 cm^{-1}. These modes are shifted and consistent with a 500 °C-annealed TiO_2 [24]. T and ST2 showed anatase modes, but ST1 did not, probably due to high Si/Ti molar rate. The presence of this phase is fundamental to give self-cleaning properties to the coatings, because anatase is the most photoactive phase of TiO_2 [12]. The photoactivity allows generating more electron-hole pairs, contributing to the enhancement of contaminant degradation mechanism and photo-induced superhydrophilicity. Both properties are crucial for superhydrophilic self-cleaning surface application [9].

The thickness and root mean square (RMS) roughness of ST1 and ST2 were assessed by AFM measurements. The thickness of ST1 and ST2 was 85 nm and 63 nm, and RMS roughness was 0.2 and 0.4 nm, respectively. The increase of $\%SiO_2$ in TiO_2/SiO_2 composite restricts the size of TiO_2 crystallites, contributing to smooth the surface [25]. This fact could explain why ST1 is smoother than ST2.

As SM has presented anti-reflexive properties, it has been characterized by ellipsometry and the values of thickness, refractive index and porosity of SM are shown in Table 4. The raw and fitting data of this analysis is available in Fig. S1.

This kind of anti-soiling coating is based on a multi-layer stack in order to provide anti-reflection properties to the system through the interference phenomenon. It has been designed based on light-matter interaction principles in thin film, so that is it possible to produce destructive interference of the light reflected at the upper and the lower interfaces in the layer/layer and layer/glass. %T was enhanced by adjusting the refractive index and thickness of each layer of the stack. The thickness of the inner film has been adjusted to ~110 nm while the thickness of external film has been optimized to ~130 nm. Refractive index of external SM film was 1.26, showing a void fraction ~43%. This film was treated with silylating agents in order to achieve hydrophobic surface, the obtained transmittance value was not significantly affected.

Table 4
Ellipsometric results of SM coating.

Sample	Thickness of inner film (nm)	Refractive of index inner film	Thickness of external film (nm)	Refractive index of external film	Porosity of external film (%)
SM	112.1	1.44	132.4	1.26	42.9

3.2. Soiling test

All the anti-soiling coatings and the uncoated glass were exposed at Belo Horizonte city (Brazil) in a very dry period (August) and ended in a rainy period (December), covering completely different weather conditions, as seen in Fig. 4a. Moreover, Fig. 4a shows the transmittance loss (%) vs time (days) measured at Belo Horizonte, revealing five different regions.

In region 1 (days 0–21), all samples have lost transmittance due to the dried weather and air pollution, resulting in high dust accumulation. In this period, ST1 and T samples had the lowest transmittance losses. In region 2 (day 28), it was observed a precipitation of less than 10 mm (see Fig. 4a) and this was sufficient to promote the glass self-cleaning. ST1 and ST2 had the best performance in this period, almost recovering initial transmittance. In region 3 (day 63), there was an extremely dried period and the samples were fouled so much, with maximum transmittance losses, reaching the value of 15.5% for uncoated glass. ST1 and ST2 had the best performance in this period too, presenting minor transmittance losses with values of 7.9% and of 10.0%, respectively. Chaba et al. (2008) also found evidence that the self-cleaning effect can occur even when the samples are not subjected to water, because the photocatalytic property of TiO_2 is active even with no precipitation [25].

After this period, a rainy period took place with precipitations of more than 20 mm (see Fig. 4a), contributing to another self-cleaning effect. In regions 4 and 5, uncoated glass presented 3.4% of transmittance loss, and only (day 91) coated glasses shown self-cleaning effect. The experimental data prove how anti-soiling coatings are effective in glass cleaning. Chaba et al. (2008) showed that organic deposits can be strongly bonded to the glass surface so that only a mechanical human intervention can washed off this deposit [25]. This explains why the uncoated glass presented a transmittance loss also after the rainy period. Based in this soiling test, it was concluded that ST1 and ST2 coatings are good candidates as self-cleaning coatings to be used on PV module cover glass, allowing reducing the transmittance losses of both in rainy and dry period. The fact that ST1 had better performances (i.e. lower transmittance losses) than ST2 could be justified in terms of surface roughness. Cuddihy (1980) listed some characteristics of the surface in order to be less susceptible to soil deposition and one of this characteristic is that the surface should be smooth, because in this way it has a lower probability to trap particles [26]. From AFM results, it was observed that ST1 presents lower RMS roughness (0.2 nm) than ST2 (0.4 nm). Jelle et al. (2012) highlighted that some PV module maintenance is necessary also when using self-cleaning coatings, owing to the fast deposition of dirt over the glasses [27]. However, the use of anti-soling coating helps in reducing the frequency of PV module maintenance. The hydrophobic sample (SM) presented worse performance with respect to the others coatings during both dry and rainy

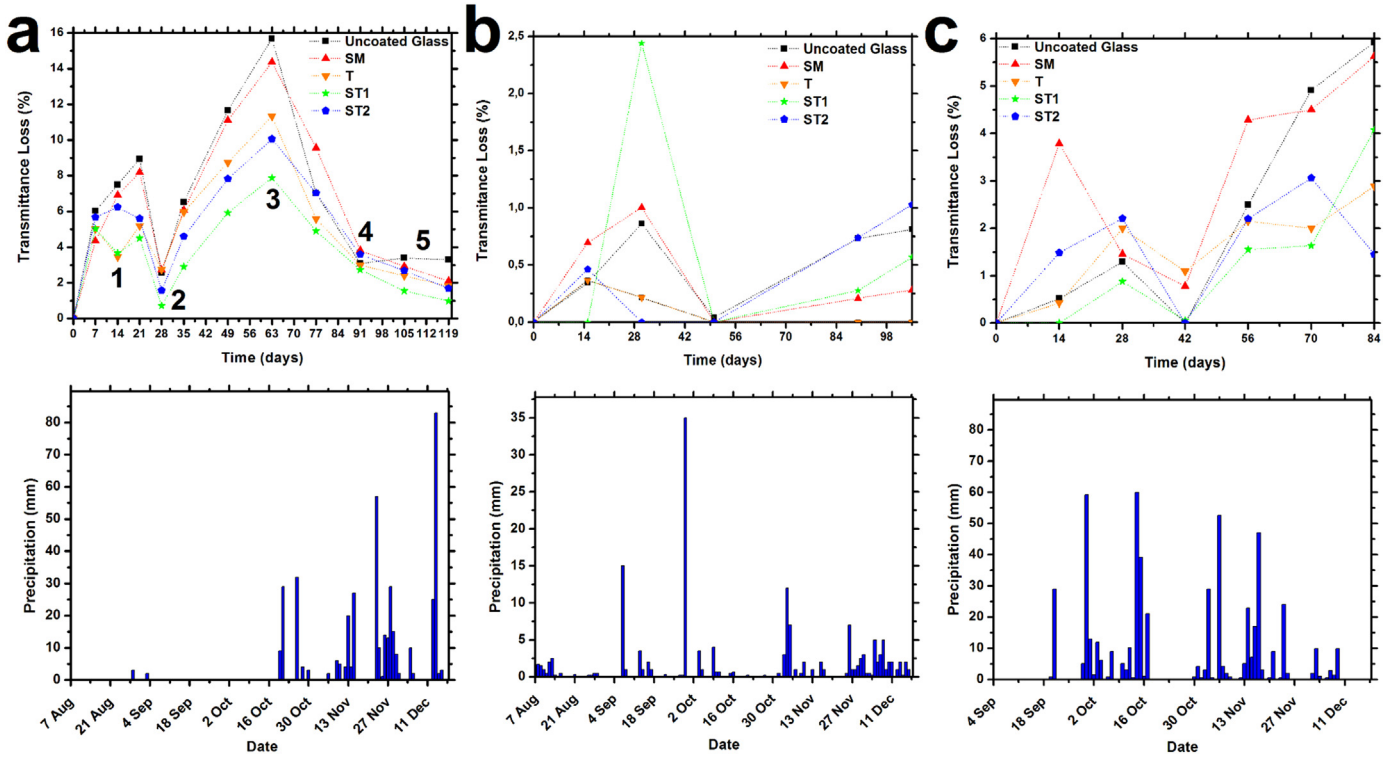

Fig. 4. Transmittance Loss (%T) vs Time (days) measured in: a) Belo Horizonte (Brazil), b) San Sebastián (Spain), c) Piacenza (Italy); and the corresponding precipitation values (mm) collected in the same period.

periods. According to Midtdal et al. (2013) glasses with these coatings require regular manual cleaning to reduce the transmittance losses, therefore they can be classified as “easy to clean” rather than self-cleaning coating [9].

The same anti-soiling coatings have been tested in San Sebastián (Spain) during the same period (August to December). However, the weather conditions in San Sebastián were completely different compared to Belo Horizonte. In particular, during the soiling test, frequent precipitations have been found, as reported in Fig. 4b. Moreover, Fig. 4b shows the transmittance loss (%T) vs time (days) measured at San Sebastián.

The soiling accumulation was very low in all the samples; therefore the optical properties were not dramatically affected. Initial transmittance loss values under 3% have been measured in all cases. As seen in Belo Horizonte, 10 mm of rainfall was sufficient to promote the cleaning of the glasses, therefore the frequent precipitation of 5–10 mm (see Fig. 4b) in San Sebastián explains the low values of transmittance losses found for all samples. As expected, the soiling effect is much less relevant in places with constant rainfall and low pollution. After 105 days, a transmittance loss under 1% was measured in most of the samples.

The same anti-soiling coatings were also tested in Piacenza (Italy) from September to December. The weather conditions in Piacenza were very similar to San Sebastián regarding the frequency of precipitation even if the volume of precipitations was higher, as reported in Fig. 4c. In spite of the higher volume of precipitations with respect to San Sebastián (more than 20 mm at 6 periods) in Italy the samples suffered of higher transmittance losses, (see Fig. 4c).

In average, ST1 presented the best performance, with the lowest transmittance losses for most of the soling test in agreement with the results obtained in Belo Horizonte. The collected data show that in spite of the fact that the soiling effect is highly dependent from the environmental conditions (e.g. rate of precipitation, local pollution, etc) the best performing anti-soling coatings maintain the performance in different locations.

As the soiling observed in Brazil and in Piacenza was strong, it was collected and then characterized. This soiling characterization is important for literature update, because most of soiling characterizations presented in the literature is regarding a particulate material from locations near to desert or sandy areas [8].

3.3. Soiling characterization

One larger uncoated glass was exposed beside the coated glasses and the deposited soiling was analyzed by SEM/EDS and Raman spectroscopy measurements. In Brazil the soiling test was carried out in a test field surrounded by high traffic roads and trees. The location of soiling test in Italy was more isolated from traffic road and near a power plant. The collected soiling was analyzed by Raman spectroscopy. In Spain the test field didn’t provide a good amount of soiling to be analyzed.

In Fig. 5 the SEM images of the collected dust in Brazil are reported and the dirtiest part of the glass was selected in order to better analyze the chemical composition of soiling by EDS.

In these images, fragments of plants, pollen, minerals, aggregates can be distinguished, that is, a mixture of organic and inorganic contaminants. The size of dust particles varied from ~1–55 μm. Particle sizes between 1 and 60 μm are commonly reported in the literature [8]. The identification of microorganisms and biofilm formation is an important issue; however it was not covered in this work as the biofilm characterization demands longer period of observation.

The EDS data of a clean LIFG glass substrate (control sample) is available in Fig. S2, revealing mainly the elements oxygen, sodium, magnesium and silicon. On the other hand, the dirty glass substrate EDS analysis presents additional elements typically present in the soil, as magnesium, aluminum, calcium, potassium and iron, Fig. 5. Gold was identified, because the glass was recovered with a gold thin film to improve SEM images. Carbon derives, probably, from amorphous carbon, soot, oil, among others. Silicon and oxygen are constituents of glass and several kinds of minerals (quartz and silicates). Aluminum, potassium, calcium and iron came from minerals, like oxides,

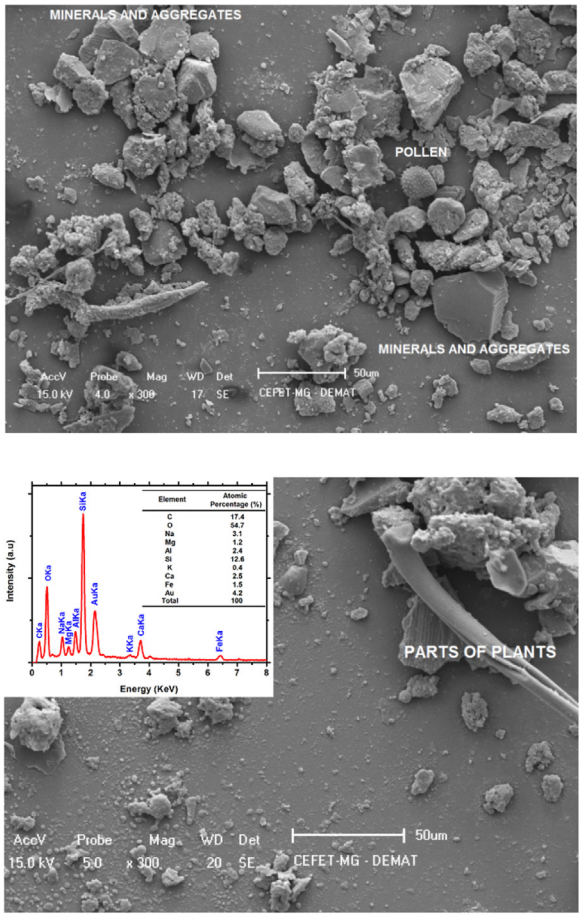

Fig. 5. SEM images of dirty glass collected in Brazil and EDS analysis of soiling chemical composition and image of the selected region. The SEM images refer to the dust analyzed in two different zones of the glass.

carbonates, silicates.

Raman analysis was performed to identify some minerals present in the dirty glass of Brazil (Fig. S3) and Italy (Fig. S4).

The soiling collected in Brazil was characterized by some minerals like hematite, calcite, goethite, mica and lepidocrocite. This composition, with a good amount of iron-based minerals, is greatly coherent with Brazilian soil, specifically in the state of Minas Gerais that is a well-known region of iron extraction. Amorphous carbon was identified too, probably originated from organic compounds, soot, industry emissions and others urban contaminations. Mica (potassium aluminosilicate) and calcite (calcium carbonate) are common minerals of Brazilian soil. This identified mineralogy is consistent with the chemical composition observed in Fig. 5. The soil collected in Italy was different from the soil found in Brazil, except regarding the calcite mineral and amorphous carbon, which were found in both locations. Moreover, albite, ilmenite and quartz minerals were identified as shown in Fig. S4. The soil in Minas Gerais is rich in iron minerals while, in Italy, calcium carbonate and silicates are the main minerals. In spite of the different soiling composition, the ST1 coating was effective to decrease the soiling effect on the module cover glass.

4. Conclusions

Anti-soiling coatings composed by superhydrophilic/hydrophobic thin films have been successfully synthesized, characterized and tested in different locations (Brazil, Italy, and Spain). Four anti-soiling coatings were proposed: TiO_2/SiO_2 superhydrophilic sol-gel films (ST1 and ST2), TiO_2 superhydrophilic e-beam evaporation film (T) and functionalized-SiO_2 hydrophobic sol-gel films (SM). TiO_2/SiO_2 films showed a persistent superhydrophilic character with water contact angles near to 0°, while functionalized-SiO_2 presented hydrophobic property. The comparative soiling tests showed the importance of setting anti-soiling strategies in region characterized by drier climate. In Brazil, which during the soiling test was characterized by a long dry period, the anti-soiling coatings were effective in reducing the soiling deposition and in the removal of the contaminants by rainwater. In the driest period, the higher transmittance loss for uncoated glass was 16%, while TiO_2/SiO_2 coating reduced of 50% this loss. In Spain and Italy, the more frequent rain precipitation made the soiling effect less relevant, however, the presence of anti-soiling coating on glass allowed to fully recover of the initial transmittance after rain washing. A chemical and mineral characterization of the soiling was carried out revealing the dependence of the contaminants from the environment conditions (e.g. car traffic, presence of industries, amount of rain and local minerals in the ground).

Acknowledgment

The authors gratefully acknowledge the support from SUN ON CLEAN project (European Commission, Call: FP7-PEOPLE-2011-IRSES, International Research Staff Exchange Scheme - MARIE CURIE ACTIONS) between CEFET-MG-Brazil, RSE-Italy, TECNALIA-Spain. The authors gratefully acknowledge the financial support of the Basque Government (project FRONTIERS ref. KK-2015/00101 and KK-2016/00093) and FAPEMIG (Minas Gerais State Agency for Research and Development).

Appendix A. Supporting information

Supplementary data associated with this article can be found in the online version at http://dx.doi.org/10.1016/j.solmat.2018.05.036.

References

[1] A. Soklič, M. Tasbihi, M. Kete, U.L. Štangar, Deposition and possible influence of a self-cleaning thin TiO2/SiO2 film on a photovoltaic module efficiency, Catal. Today 252 (2015) 54–60.
[2] M.R. Maghami, H. Hizam, C. Gomes, M.A. Radzi, M.I. Rezadad, S. Hajighorbani, Power loss due to soiling on solar panel: a review, Renew. Sustain. Energy Rev. 59 (2016) 1307–1316.
[3] A. Rao, R. Pillai, M. Mani, P. Ramamurthy, Influence of dust deposition on photovoltaic panel performance, Energy Procedia 54 (2014) 690–700.
[4] S. Mekhilef, R. Saidur, M. Kamalisarvestani, Effect of dust, humidity and air velocity on efficiency of photovoltaic cells, Renew. Sustain. Energy Rev. 16 (2012) 2920–2925.
[5] F. Mejia, J. Kleissl, J.L. Bosch, The effect of dust on solar photovoltaic systems, Energy Procedia 49 (2014) 2370–2376.
[6] V. Sharma, S.S. Chandel, Performance and degradation analysis for long term reliability of solar photovoltaic systems: a review, Renew. Sustain. Energy Rev. 27 (2013) 753–767.
[7] S.A. Sulaiman, A.K. Singh, M.M.M. Mokhtar, M.A. Bou-Rabee, Influence of dirt accumulation on performance of PV panels, Energy Procedia 50 (2014) 50–56.
[8] T. Sarver, A. Al-Qaraghuli, L.L. Kazmerski, A comprehensive review of the impact of dust on the use of solar energy: history, investigations, results, literature, and mitigation approaches, Renew. Sustain. Energy Rev. 22 (2013) 698–733.
[9] K. Midtdal, B.P. Jelle, Self-cleaning glazing products: a state-of-the-art review and future research pathways, Sol. Energy Mater. Sol. Cells 109 (2013) 126–141.
[10] S.C.S. Costa, A.S.A.C. Diniz, L.L. Kazmerski, Dust and soiling issues and impacts relating to solar energy systems: literature review update for 2012–2015, Renew. Sustain. Energy Rev. 63 (2016) 33–61.
[11] M.A. Bahattab, I.A. Alhomoudi, M.I. Alhussaini, M. Mirza, J. Hegmann, W. Glaubitt, P. Löbmann, Anti-soiling surfaces for PV applications prepared by sol-gel processing: comparison of laboratory testing and outdoor exposure, Sol. Energy Mater. Sol. Cells 157 (2016) 422–428.
[12] K. Nakata, A. Fujishima, TiO2 photocatalysis: design and applications, J. Photochem. Photobiol. C: Photochem. Rev. 13 (2012) 169–189.
[13] M.A.M.Ld Jesus, J.Td.S. Neto, G. Timò, P.R.P. Paiva, M.S.S. Dantas, Ad.M. Ferreira, Superhydrophilic self-cleaning surfaces based on TiO2 and TiO2/SiO2 composite films for photovoltaic module cover glass, Appl. Adhes. Sci. 3 (2015).
[14] Ö. Kesmez, H. Erdem Çamurlu, E. Burunkaya, E. Arpaç, Sol–gel preparation and characterization of anti-reflective and self-cleaning SiO2–TiO2 double-layer nanometric films, Sol. Energy Mater. Sol. Cells 93 (2009) 1833–1839.
[15] L. Ye, Y. Zhang, X. Zhang, T. Hu, R. Ji, B. Ding, B. Jiang, Sol–gel preparation of

SiO2/TiO2/SiO2–TiO2 broadband antireflective coating for solar cell cover glass, Sol. Energy Mater. Sol. Cells 111 (2013) 160–164.
[16] Y.J. Xu, J.X. Liao, Q.W. Cai, X.X. Yang, Preparation of a highly-reflective TiO2/SiO2/Ag thin film with self-cleaning properties by magnetron sputtering for solar front reflectors, Sol. Energy Mater. Sol. Cells 113 (2013) 7–12.
[17] M. Houmard, G. Berthomé, J.C. Joud, M. Langlet, Enhanced cleanability of super-hydrophilic TiO2–SiO2 composite surfaces prepared via a sol–gel route, Surf. Sci. 605 (2011) 456–462.
[18] S. Liu, X. Liu, S.S. Latthe, L. Gao, S. An, S.S. Yoon, B. Liu, R. Xing, Self-cleaning transparent superhydrophobic coatings through simple sol–gel processing of fluoroalkylsilane, Appl. Surf. Sci. 351 (2015) 897–903.
[19] Y.-Y. Quan, L.-Z. Zhang, Experimental investigation of the anti-dust effect of transparent hydrophobic coatings applied for solar cell covering glass, Sol. Energy Mater. Sol. Cells 160 (2017) 382–389.
[20] S. Sutha, S. Suresh, B. Raj, K.R. Ravi, Transparent alumina based superhydrophobic self–cleaning coatings for solar cell cover glass applications, Sol. Energy Mater. Sol. Cells 165 (2017) 128–137.
[21] C. Agustín Sáenz, O. Zubillaga Alcorta, M. Brizuela Parra, A broadband anti-reflective sol-gel coating composition, Patent application EP17382016, 2017.
[22] T.P. Ang, C.S. Toh, Y.-F. Han, Synthesis, characterization, and activity of visible-light-driven nitrogen-doped TiO2-SiO2 mixed oxide photocatalysts, J. Phys. Chem. C 113 (2009) 10560–10567.
[23] S. Permpoon, M. Houmard, D. Riassetto, L. Rapenne, G. Berthomé, B. Baroux, J.C. Joud, M. Langlet, Natural and persistent superhydrophilicity of SiO2/TiO2 and TiO2/SiO2 bi-layer films, Thin Solid Films 516 (2008) 957–966.
[24] W.F. Zhang, Y.L. He, M.S. Zhang, Z. Yin, Q. Chen, Raman scattering study on anatase TiO2 nanocrystals, J. Phys. D: Appl. Phys. 33 (2000) 912–916.
[25] A. Chabas, T. Lombardo, H. Cachier, M.H. Pertuisot, K. Oikonomou, R. Falcone, M. Verità, F. Geotti-Bianchini, Behaviour of self-cleaning glass in urban atmosphere, Build. Environ. 43 (2008) 2124–2131.
[26] E.F. Cuddihy, Theoretical considerations of soil retention, Sol. Energy Mater. 3 (1980) 21–33.
[27] B.P. Jelle, A. Hynd, A. Gustavsen, D. Arasteh, H. Goudey, R. Hart, Fenestration of today and tomorrow: a state-of-the-art review and future research opportunities, Sol. Energy Mater. Sol. Cells 96 (2012) 1–28.